

Simulation Program Verification and Performance Prediction of the Multi-type Heat Pump System

Doyoung Han*, Kwanjun Park** and Hanhong Lee**

Key words: Multi-type heat pump system, System simulation program, System design, Performance prediction

Abstract

The simulation program which can predict major performances of the multi-type heat pump system was developed. In order to verify the simulation program, several experimental tests were performed under various recommended conditions. The experimental results show in good agreement with simulation results. The verified simulation program was used to analyze the system performance. The capacities and the COP's under the various indoor and outdoor conditions were predicted. Therefore, it may be concluded that the system simulation program developed in this study may be effectively used for the system design and the performance prediction of the multi-type heat pump system.

Nomenclature

A : heat transfer area [m^2]
 c_p : specific heat [$\text{J}/\text{kg} \cdot \text{K}$]
 h : enthalpy [J/kg]
 \dot{m} : mass flow rate [kg/s]
 P : pressure [N/m^2]
 T : temperature [$^{\circ}\text{C}$]
 \dot{W} : compressor power [W]

Greek symbols

δ : fin thickness [m]
 ϵ : effectiveness of heat exchanger
 ρ : density [m^3/kg]
 ν : specific volume [kg/m^3]

Subscript

f : friction coefficient

1. Introduction

In recent years, maintenance of comfortable indoor conditions has been a very important area of air-conditioning system. At the same time, controllability of conditioned room and en-

* Member of SAREK, Professor in the Department of Mechanical Engineering, Kookmin University, Seoul 136-702, Korea

** Graduate School of Mechanical Engineering, Kookmin University, Seoul 136-702, Korea

ergy saving have also been important issues.⁽¹⁾ To satisfy this purpose, system design techniques and performance prediction methods have been developed. The multi-type heat pump system, which consists of several indoor units, is considered important in the multiple space air-conditioning system. For this system, it is very important to develop the system design technique and optimal control strategy of the overall system.⁽²⁾

In this study, the simulation program, which can predict the major system parameters such as cooling and heating capacity, power consumption, and coefficient of performance for the multi-type heat pump system, was developed. And the simulation program was verified through several experimental tests. Therefore, the developed simulation program may be effectively used for designing and analyzing the multi-type heat pump system.

2. Mathematical models

Fig. 1 represents the schematic diagram of multi-type heat pump system. As shown in this figure, system is composed of two major units: One is an outdoor unit, which consists of compressor, oil separator, four-way valve, outdoor heat exchanger, receiver tank, accumulator, and electronic expansion valve. Others are four indoor units which consist of electronic expansion valves, and indoor heat exchangers. Cooling or heating mode is deter-

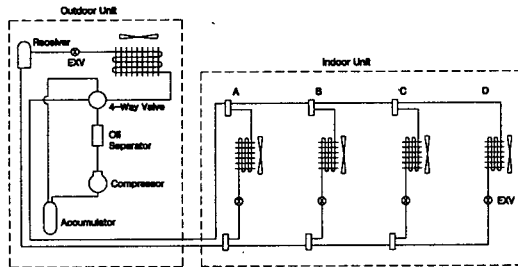


Fig. 1 Schematic diagram of multi-type heat pump system.

mined by a reversing four-way valve.

The compressor manufacturer's data may be used for the development of the compressor model. The power consumption ($\dot{W}_{cm, actual}$) and the mass flow rate ($\dot{m}_{r, actual}$) of compressor are calculated as follows;

$$\dot{W}_{cm, actual} = \left[\frac{\dot{m}_{r, actual}}{\dot{m}_{r, map}} \right] \left[\frac{\Delta h_{isen, actual}}{\Delta h_{isen, map}} \right] \dot{W}_{cm, map} \quad (1)$$

$$\dot{m}_{r, actual} = \left[1 + 0.75 \left(\frac{\nu_{map}}{\nu_{actual}} - 1 \right) \right] \dot{m}_{r, map} \quad (2)$$

where ν and Δh represent specific volume and enthalpy change, respectively.

The air-side area⁽³⁾ of finned-tube heat exchanger is equal to the sum of the area of fin and tube in contact with air. It may be calculated as follows;

$$\begin{aligned} A_a &= A_f + A_{tubes} \\ &= 2L \cdot FP \cdot NR \left[ST \cdot WT - \frac{\pi Do^2}{4} \right] \\ &\quad + NR \cdot \pi Do \cdot L_{ex} \end{aligned} \quad (3)$$

where L represents horizontal length of tube, FP the number of fins per unit length, NR the number of tubes, ST vertical length between tubes, WT horizontal length between tubes, Do tube surface diameter, and L_{ex} tube horizontal length.

The free flow frontal area of finned-tube heat exchanger may be calculated as follows;

$$A_{free-flow} = A_{fr} - A_{tubes}^* - A_f^* \quad (4)$$

$$A_{fr} = H \cdot L \quad (5)$$

$$A_{tubes}^* = NV \cdot Do \cdot L_{ex} \quad (6)$$

$$A_f^* = NF \cdot H \cdot \delta \quad (7)$$

where A_{fr} , A_{tubes}^* , and A_f^* are the air flow areas of heat exchanger, tube, and fin, re-

spectively. H denotes vertical height, NV the number of horizontal tubes, NF the number of fins, and δ the thickness of fin. The ratio of air-side heat transfer area and free flow frontal area in finned-tube heat exchanger may be calculated as follows;

$$A_{\min} = \frac{A_a}{A_{\text{free-flow}}} \quad (8)$$

Heat transfer rate using ε -Ntu method between refrigerant and air in heat exchanger may be calculated as follows;

$$Q = \varepsilon (mc_p)_{\min} (T_{h,in} - T_{c,in}) \quad (9)$$

where $(mc_p)_{\min}$ denotes smaller value of mass multiplied by specific heat, and $T_{h,in}$ and $T_{c,in}$ denote the inlet temperature of high and low temperature side. The expansion devices in the

multi-type heat pump system are modeled as electronic expansion valves⁽⁵⁾ which control the superheat temperature of the evaporator outlet at the specified control ranges.

The pressure losses at the refrigerant line may be calculated by

$$\Delta P = \frac{2f \frac{L_e}{D} \dot{m}^2}{\rho_m} \quad (10)$$

where f is the Moody friction factor, and L_e , D , and ρ_m denote equivalent length, the diameter and average density, respectively.

Fig. 2 shows the calculation procedure of the simulation program for the multi-type heat pump system in the cooling mode. The dry-bulb temperature of indoor and outdoor air, the superheat value of the evaporator, and the subcooled value of the condenser are assumed. After compressor and condenser subroutines are completed, inlet refrigerant temperature in expansion valve is calculated. This procedure continues until E_1 reaches the specified boundary, where E_1 is the error between previous and present refrigerant temperature at expansion valve. If E_1 reaches less than 1%, each outlet refrigerant temperature in evaporators is calculated. In order to make E_2 , the error between previous and present refrigerant temperature at evaporators, converge to 1%, each refrigerant flow rate is recalculated and redistributed. To make the error between the refrigerant flow rate at compressor and the sum of refrigerant flow rate at evaporators converge within 1%, low side pressure is adjusted.

Fig. 3 shows simulation procedure in the heating mode. As shown in this figure, several initial conditions are assumed. After all the calculations at compressor and condenser are completed, outlet pressure of condenser is calculated. This procedure continues until E_3 , which is the error between outlet pressure at condenser and average pressure at distributed tube, reaches the specified boundary. If the error

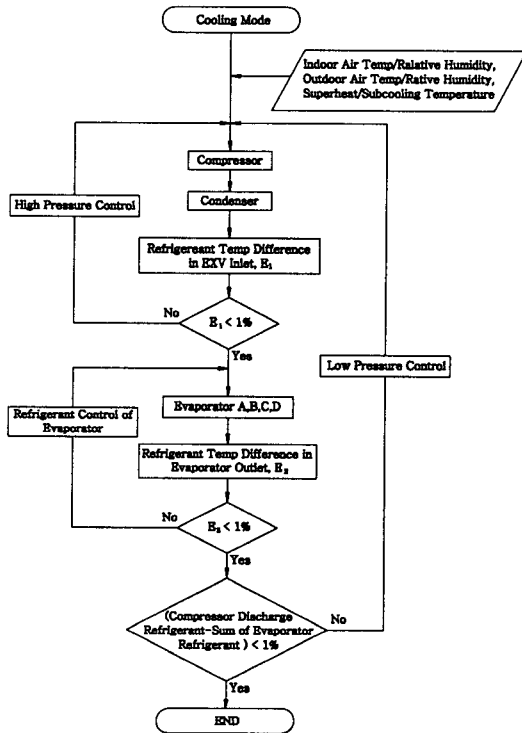


Fig. 2 Cooling mode simulation flow chart.

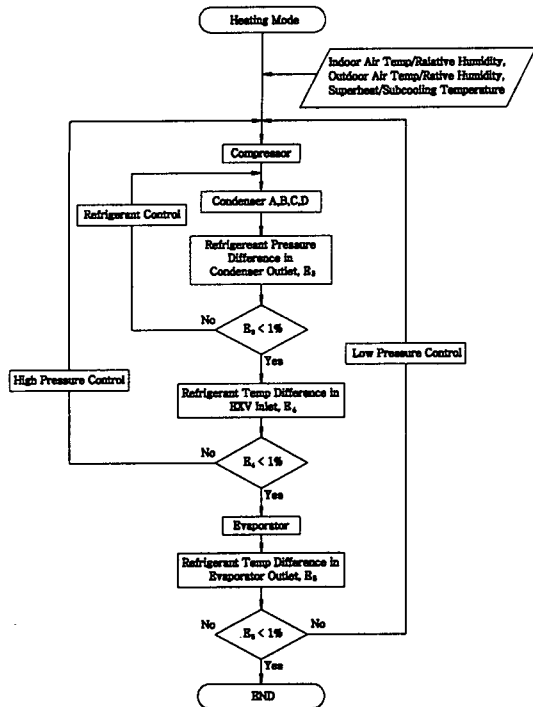


Fig. 3 Heating mode simulation flow chart.

does not converge to less than 1%, each refrigerant flow rate is recalculated and redistributed. High side pressure is readjusted to make E_4 , the difference between previous and current inlet refrigerant temperature at expansion device, converge within 1%. Outlet temperature at evaporator is calculated. If E_5 does not converge to less than 1%, low side pressure is readjusted.

3. Model verification

Table 1 represents the specification of multi-type heat pump system. To validate the computer simulation program, multi-type heat pump system is designed⁽⁷⁾ and tested. For the experimental test, dynamic environmental chamber is designed and constructed. The environmental chamber⁽⁸⁾ consists of four indoor chambers and an outdoor chamber. Table 2 shows test conditions used for the verification of multi-type heat pump simulation. The comparison of simulation and experimental results are shown

Table 1 Specifications of multi-type heat pump system

Outdoor unit	Compressor	Capacity; 18,000 kcal/h
	Heat exchanger	Finned-tube type Frontal area; 1.2619 m ² 2 Rows, 40 Steps, 5 Circuits
	Fan	Propeller fan Air flow rate; 110 m ³ /min
	Expansion device	Electronic expansion valve
Indoor unit	Heat exchanger	Finned-tube type Frontal area; 0.3337 m ² 1 Rows, 8 Steps, 2 Circuits
	Fan	Turbo fan Air flow rate; 18 m ³ /min
	Expansion device	Electronic expansion valve

Table 2 Test conditions

		Cooling mode			Heating mode		
		Normal	Over-load	Low-temp	Normal	Over-load	
Outdoor unit		Temp(°C)	35	44	21	7	21
		RH(%)	45	25	55	85	55
Indoor unit	A	Temp(°C)	27	31	21	20	24
		RH(%)	55	35	55	50	50
	B	Temp(°C)	27	32	20	22	23
		RH(%)	55	35	55	50	50
	C	Temp(°C)	28	33	22	22	23
		RH(%)	55	35	55	50	50
	D	Temp(°C)	27	32	21	21	24
		RH(%)	55	35	55	50	50

Table 3 Test and simulation results in cooling mode

Cooling capacity (kcal/h)		Normal			Overload			Low temp.		
		Experimental	Simulation	Error(%)	Experimental	Simulation	Error(%)	Experimental	Simulation	Error(%)
Indoor unit	A	3050	3266	7.1	3079	3076	-0.1	3020	3097	2.5
	B	3030	2959	-2.3	3159	3248	2.8	2850	2905	1.9
	C	2950	3128	6.0	2765	2845	2.9	2460	2614	6.3
	D	2900	3132	8.0	2277	2692	18.2	2050	2413	17.7
COP		3.08	3.24	5.2	2.38	2.51	5.5	2.94	3.20	8.8

Table 4 Test and simulation results in heating mode

Heating capacity (kcal/h)		Normal			Overload		
		Experimental	Simulation	Error(%)	Experimental	Simulation	Error(%)
Indoor unit	A	3200	3607	12.7	4300	4322	0.5
	B	2950	3117	5.7	4100	4342	5.9
	C	2900	2848	-1.8	4000	3760	-6.0
	D	2500	2711	8.4	3750	3537	-5.7
COP		3.74	4.02	7.5	4.08	4.23	3.7

in Table 3 and Table 4 for cooling mode and heating mode.

Test results are compared with the simulation results for cooling capacities and COP's. In the normal test condition, error is 4.7% in capacity and 5.2% in COP. In the overload condition, error is 6.0% in capacity and 5.5% in COP. In the low-temperature condition, error is 7.1% in capacity and 8.8% in COP. In the case of the overload and the low-temperature condition, error at the indoor unit D, which is located at the remotest location, is relatively larger than the others. This may be due to insufficient refrigerant flow at the unit D.

Test and simulation results are also compared for heating capacity and COP. In the normal test condition, error is 6.3% in capacity and 7.5% in COP. In the overload condition, error is -1.3% in capacity and 3.7% in COP.

4. Performance prediction

Experimental results are compared with the simulation results to validate the computer simulation program over a wide range of cooling and heating conditions. The verified program is

used to predict the performance of multi-type heat pump system.

4.1 Capacity and C.O.P with varying air temperature

Fig. 4 and Fig. 5 show the average cooling capacity and cooling COP. The indoor air temperature is 24°C, 27°C, and 30°C at 55% relative humidity. The outdoor air temperature is 32°C, 35°C, 38°C, and 43°C at 45% relative humidity.

When outdoor air temperature is constant, and indoor air temperature increases, cooling

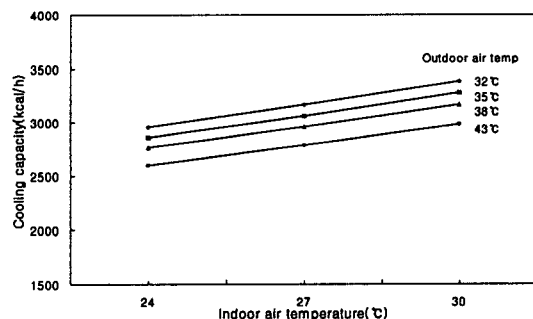


Fig. 4 Cooling capacity w.r.t. the indoor and the outdoor air temperature.

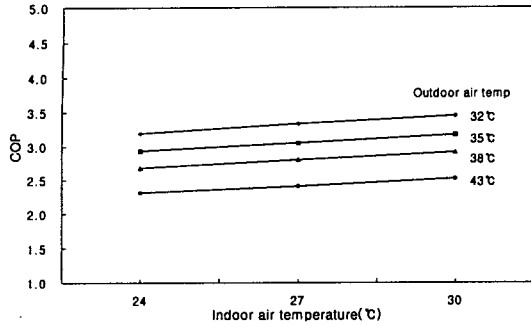


Fig. 5 Cooling COP w.r.t. the indoor and the outdoor air temperature.

capacity and COP increase. When indoor air temperature is constant, and outdoor air temperature increases, cooling capacity and COP decrease.

Fig. 6 and Fig. 7 show the average heating capacity and heating COP. The indoor air temperature is 18°C, 21°C, and 24°C at 50% rela-

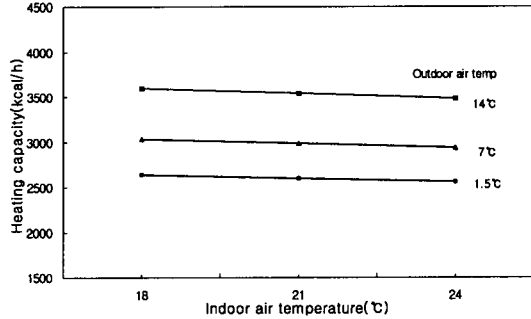


Fig. 6 Heating capacity w.r.t. the indoor and the outdoor air temperature.

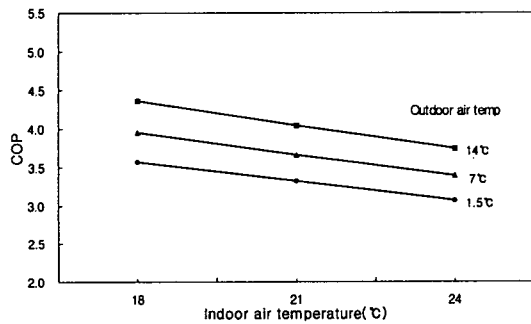


Fig. 7 Heating COP w.r.t. the indoor and the outdoor air temperature.

tive humidity. The outdoor air temperature is 1.5°C, 7°C, and 14°C at 45% relative humidity.

In the heating mode, when outdoor air temperature is constant, and indoor air temperature increases, heating capacity and COP decrease. When indoor air temperature is constant, and outdoor air temperature increases, heating capacity and COP increase.

4.2 Capacity and C.O.P with air flow rate change

To analyze the system performance at different air flow rate, 14 m³/min, 16 m³/min, and 18 m³/min are selected as the indoor air flow rates while 60 m³/min, 85 m³/min, and 110 m³/min are selected as the outdoor air flow rates.

4.2.1 The change of indoor air flow rate

Fig. 8 and Fig. 9 show the average cooling

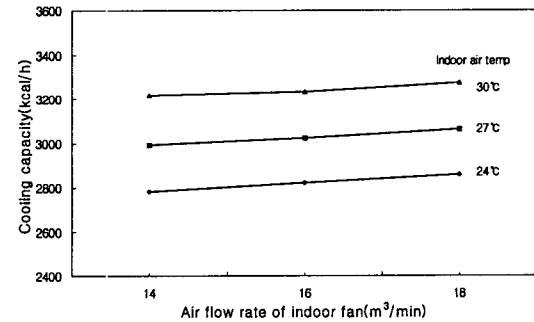


Fig. 8 Cooling capacity w.r.t. the indoor fan air flow rate.

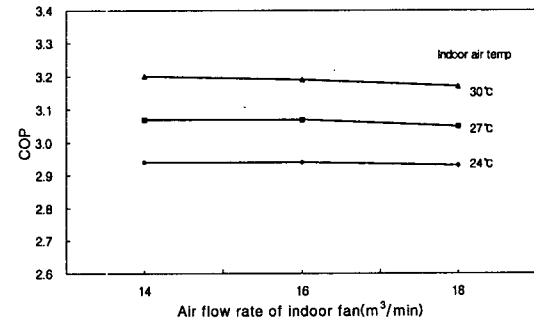


Fig. 9 Cooling COP w.r.t. the indoor fan air flow rate.

capacity and the cooling COP with respect to indoor air flow rates for the indoor air temperature 24°C, 27°C, and 30°C at 55% relative humidity. When the indoor air temperature is constant and the indoor air flow rates increases, the cooling capacity increases but the COP decreases. When the indoor air flow rate is constant and the indoor air temperature increases, the cooling capacity and the COP increase.

Fig. 10 and Fig. 11 show the average heating capacity and the heating COP with respect to indoor air flow rates for indoor air temperature 18°C, 21°C, and 24°C at 50% relative humidity. Outdoor air temperature and relative humidity is 7°C and 85%. When the indoor air temperature is constant and the indoor air flow rate increases, cooling capacity and COP increase. When the indoor air flow rate is constant and the indoor air temperature increases,

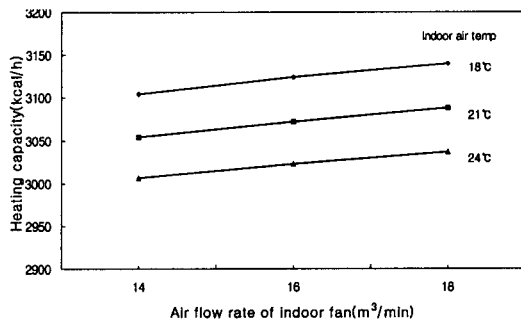


Fig. 10 Heating capacity w.r.t. the indoor fan air flow rate.

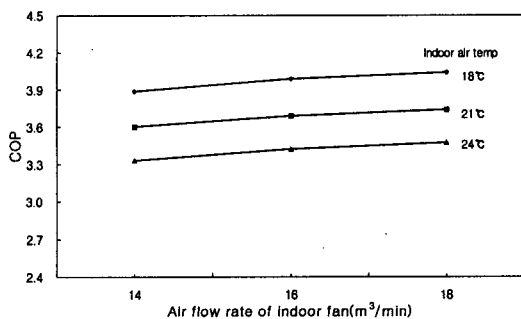


Fig. 11 Heating COP w.r.t. the indoor fan air flow rate.

the heating capacity and the COP decrease.

4.2.2 The change of outdoor air flow rate

Fig. 12 and Fig. 13 show the average cooling capacity and the cooling COP with respect to the outdoor air flow rates for the outdoor air temperature 32°C, 35°C, 38°C, and 43°C at the 45% relative humidity. The indoor air temperature and the relative humidity are 27°C and 55% respectively. When the outdoor air temperature is constant and the air flow rate increases, cooling capacity and COP increase.

When the air flow rate is constant but the outdoor air temperature increases, cooling capacity and COP decrease.

Fig. 14 and Fig. 15 show the average heating capacity and the heating COP with respect to the outside air flow rates for outdoor air temperature 1.5°C, 7°C, and 14°C

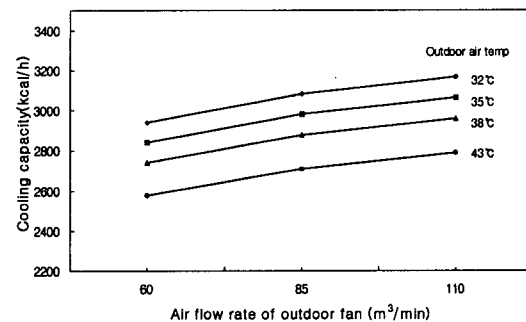


Fig. 12 Cooling capacity w.r.t. the outdoor fan air flow rate.

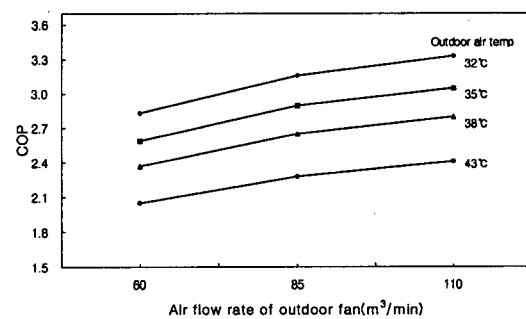


Fig. 13 Cooling COP w.r.t. the outdoor fan air flow rate.

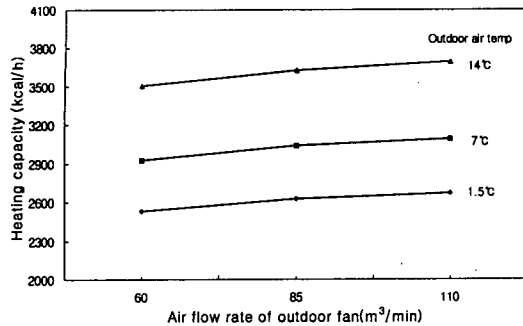


Fig. 14 Heating capacity w.r.t. the outdoor fan air flow rate.

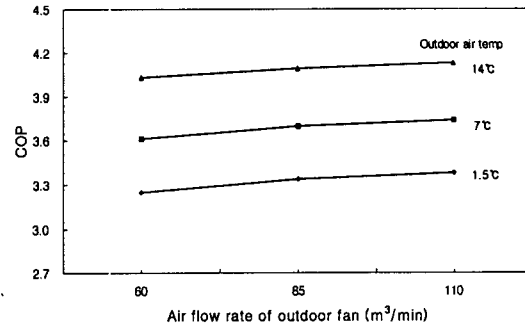


Fig. 15 Heating COP w.r.t. the outdoor fan air flow rate.

at the 85% relative humidity. The indoor air temperature and the relative humidity are 21°C and 50%, respectively. As shown in these figures, when the outdoor air temperature is constant and the air flow rate increases, the heating capacity and the COP increase. When the air flow rate and the outdoor air temperature increase, heating capacity and COP increase.

5. Conclusions

The results of this research may be summarized as follows:

(1) The simulation models for the multi-type heat pump system, which consists of one outdoor unit and four indoor units, are developed, and the system simulation program is developed.

(2) A multi-type heat pump system is designed by using computer simulation program and constructed. Experimental tests are performed under the wide ranges of conditions, such as the normal load test condition, the overload condition and the low temperature condition. Test results are compared with simulation results, and the simulation results are in agreements with test results.

(3) The system performance of a multi-type heat pump system is predicted by using the verified simulation program. The developed simulation program may be used for the design and the performance prediction of the multi-

type heat pump system.

References

1. Han, D., 1999, The development of multi-type air conditioning system, Report, Ministry of Commerce, Industry and Energy.
2. Han, D. and Kwon, H., 1999, Zone temperature control of the multi-type heat pump system, Proceedings of SAREK, Vol. 2, pp. 611-616.
3. McQuiston, F. C., 1981, Finned tube heat exchangers; state of the art for the air side, ASHRAE Transactions, Vol. 87, Pt. 1.
4. He, X., 1997, Modeling of vapor compression cycle for multivariable feedback control of HVAC systems, ASME, Vol. 119.
5. Han, D. and Park, K., 1997, Design and performance analysis of water-to-air heat pump system, Korean journal of Air-Conditioning and Refrigeration Engineering, Vol. 9, No. 4, pp. 462-471.
6. Steven, C. C. and Raymond, P. C., 1990, Numerical methods for engineers, McGraw-Hill.
7. Han, D., Kwon, H. and Ha, S., 1999, Design and performance prediction of the multi-type heat pump system, Proceedings of SAREK, Vol. 2, pp. 515-520.
8. Han, D. and Kim, K., 1998, Design and control of dynamic environmental chamber, Proceedings of SAREK, Vol. 2, pp. 656-661.